Effect of RNA Secondary Structure on the Kinetics of DNA Synthesis Catalyzed by HIV-1 Reverse Transcriptase†

Zucai Suo and Kenneth A. Johnson*

Department of Biochemistry and Molecular Biology, 106 Althouse Laboratory, The Pennsylvania State University, University Park, Pennsylvania 16802

Received May 23, 1997; Revised Manuscript Received July 29, 1997⊗

ABSTRACT: The effect of RNA secondary structure on the kinetics of DNA synthesis catalyzed by HIV-1 RT was determined using a 66 nucleotide RNA template containing a stable 12 base pair hairpin structure. Prior to reaching the hairpin structure, the primer elongation by RT was fast and the kinetics of polymerization was not affected by the presence of the secondary structure. Once within the regions of template secondary structure, polymerization was much slower and RT paused at five distinct sites [Suo, Z., & Johnson, K. A. (1997) *Biochemistry* (manuscript submitted for publication)]. Kinetic analysis of single nucleotide incorporation at the pause sites showed polymerization occurred by both a fast phase (54−76 s^{-1}) and a slow phase (0.07−0.4 s^{-1}) during a single binding event. The biphasic kinetics suggests that the DNA substrates are initially bound in both productive and nonproductive states at the polymerase site of RT. The nonproductively bound DNA is slowly converted into a productive state without dissociation from the enzyme. At the pause sites, the enzyme amplitudes of the fast phase are small (4.0−15%) while the amplitudes of the slow phase are large (11−40%). In contrast, only the reaction at the fast phase was observed at the nonpause sites and the enzyme amplitudes were large (63−66%) although the nucleotide incorporation rates (62−78 s^{-1}) are similar to the fast phase rates at the pause sites. These indicate that DNA substrates were bound predominantly nonproductively at pause sites and productively at nonpause sites. However, the overall binding affinity of DNA substrates was measured by the nitrocellulose-DEAE double filter binding assay, binding affinity at both pause sites and nonpause sites was similar (9−38 nM). This indicates that substrates are bound tightly at the large binding cleft of HIV-1, although they may not be productively bound at the polymerase active site. These results and those reported elsewhere [Suo, Z., & Johnson, K. A. (1997) *Biochemistry* (manuscript submitted for publication)] are consistent with a model in which, at pause sites, HIV-1 RT remains bound to DNA substrates waiting for the melting of the next stem base pair of template secondary structure. Upon melting of the stem base pair, polymerization to fill the open template site is fast and largely irreversible, allowing RT to read through the stable hairpin structures.

Virally encoded reverse transcriptase (RT)[1] catalyzes the replication of human immunodeficiency virus (HIV) (Rey *et al.*, 1984; Hoffman *et al.*, 1985). The enzyme catalyzes RNA-dependent DNA polymerization, DNA-dependent DNA polymerization, and RNase H degradation of the RNA/DNA heteroduplex (Huber *et al.*, 1989; Le Grice, 1993). HIV-1 RT is a tightly associated heterodimer of a 66 kDa polypeptide (p66) and a 51 kDa polypeptide (p51). The p66 subunit possesses both polymerase and RNase H activities while the p51 lacks RNase H domain and its DNA polymerase active site is buried and not accessible (Hansen *et al.*, 1980; Jacobo-Molina *et al.*, 1993; Kohlstaedt *et al.*, 1992).

During HIV-1 replication, RT copies the RNA viral strand into a minus-strand DNA and then uses this DNA to synthesize a plus-strand DNA. It has been found that RT pauses in runs of template rGs and rCs during minus-strand synthesis, and in most runs of template dTs and dAs during plus-strand synthesis (Klarmann *et al.*, 1993). Strong hindrance of reverse transcription catalyzed by HIV-1 RT *in vitro* has been observed at the putative secondary structures of both RNA and DNA templates (Dudding *et al.*, 1991; Klarmann *et al.*, 1993; Olsen *et al.*, 1994; Pop & Biebricher, 1996). Two general mechanisms have been proposed by which RT might pause at a particular template position (Klarmann *et al.*, 1993). First, RT may remain bound to the primer template with polymerization through pause sites at rates that are much slower than the polymerization rates at nonpause sites. Second, RT may dissociate from the primer template at sites of RNA secondary structure so that pause sites accumulate in solution. It also has been suggested that the binding of DNA to RT forms either an inactive "outer" binary complex or an active "inner" one, and pause occurs when the outer form dominates (Pop & Biebricher, 1996).

In this report, we explore, by transient kinetic methods, the mechanistic basis for pausing of DNA synthesis when HIV-1 RT reads through RNA template secondary structure. Using a 66 nucleotide RNA template derived from HIV-1 genome, we have revealed that HIV-1 RT strongly paused at five positions during DNA synthesis through the template hairpin (Suo & Johnson, 1997b). The mechanistic basis of polymerization pausing is reported.

† This work is supported by National Institutes of Health Grant GM44613 (to K.A.J.).

* Author to whom correspondence should be addressed. Tel: (814) 865-1200. Fax: (814) 865-3030. Email: kaj1@psu.edu.

⊗ Abstract published in *Advance ACS Abstracts,* September 15, 1997.

[1] Abbreviations: dNTP, 2′-deoxynucleotide 5′-triphosphate; HIV-1, human immunodeficiency virus type 1; RT, reverse transcriptase.

S0006-2960(97)01217-8 CCC: $14.00

Table 1: DNA Primers

20-mer	TGTTGGCTCTGGTCTGCTCT
25-mer	TGTTGGCTCTGGTCTGCTCTGAAGA
32-mer	TGTTGGCTCTGGTCTGCTCTGAAGAAAATTCC
35-mer	TGTTGGCTCTGGTCTGCTCTGAAGAAAATTCCCTG
36-mer	TGTTGGCTCTGGTCTGCTCTGAAGAAAATTCCCTGG
37-mer	TGTTGGCTCTGGTCTGCTCTGAAGAAAATTCCCTGGC
47-mer	TGTTGGCTCTGGTCTGCTCTGAAGAAAATTCCCTGGCCTTCCCTTGT
48-mer	TGTTGGCTCTGGTCTGCTCTGAAGAAAATTCCCTGGCCTTCCCTTGTA

MATERIALS AND METHODS

Protein Expression and Purification. HIV-1 wild-type RT was purified from *Escherichia coli* 6222/pDMI,1/pRT$_{66/51}$ (Muller *et al.*, 1989) by the procedure of Kati *et al.* (1992), with one exception. Following Q-Sepharose chromatography, peak fractions were pooled and dialyzed against 10 mM NaCl/Buffer A (50 mM Tris-Cl, pH 7.9, 2 mM EDTA, 2 mM DTT, and 10% glycerol). Protein (20 mg) was loaded onto a Mono S 5/5 column (Pharmacia) equilibrated with 10 mM NaCl/Buffer A (Stahlhut *et al.*, 1994). After washing with 10 mM NaCl/Buffer A, the column was eluted with a three-step gradient at a flow rate of 0.65 mL/min: 10 to 118 mM NaCl/Buffer A over 40 min; 118 mM NaCl/Buffer A over 20 min; and 118−500 mM NaCl/Buffer A over 40 min. RT started to elute at 55 mM NaCl. Peak fractions were collected and analyzed by SDS−PAGE gel. The gel was stained with Coomassie Blue and the ratio of the two subunit bands (p66/p51) was quantitated using a PDSI densitometer (Molecular Dynamics, Sunnyvale, CA). Fractions with ratios (p66/p51) larger than 1.0 were pooled. After dialysis against 10 mM NaCl/Buffer A, the protein was passed through the Mono S 5/5 column a second time. Peak fractions were collected, concentrated, and dialyzed against 50 mM NaCl/Buffer A containing 50% glycerol. RT was stored at −80 °C. The ratio of the Coomassie Blue staining intensities of the two bands suggested a final subunit composition of 1.3:1.0 (p66/p51). The protein concentration was determined spectrophotometrically at 280 nm, with the extinction coefficients 136 270 and 124 180 M^{-1} cm^{-1} for p66 and p51 subunits, respectively. All concentrations of RT reported in this paper were determined spectrophotometrically.

The purified wild-type RT was shown to be approximately 70% active by active site titration measuring the incorporation of a single dATP to the 25/45-mer DNA/DNA duplex (data not shown). The 20% increase in enzyme active site concentration over previous preparation (Kati *et al.*, 1992) is due to the removal of excess p51 by Mono S column, thereby increasing the ratio of two subunits (p66/p51) from 1.0:1.24 to 1.3:1.0. Notably, if we used the extinction coefficient of 334 000 M^{-1} cm^{-1} for the heterodimer to estimate RT concentration, which was used by Reardon (1992), the enzyme would be approximately 90% active.

Chemicals. [γ-^{32}P]ATP was purchased from ICN. dNTPs were purchased from Pharmacia. Biospin columns were purchased from Bio-Rad. Diethyl pyrocarbonate and molecular biology grade reagents, including acrylamide, TBE buffer, EDTA, Tris-Cl buffer, and sodium acetate, were purchased from Sigma.

Synthetic Oligonucleotides. RNA template of 66 nucleotides was synthesized by runoff transcription by T7 RNA polymerase using an AmpliScribe T7 high-yield transcription kit from Epicentre Technologies according to manufacturer's instructions. The RNA was dephosphorylated with calf intestine alkaline phosphatase (New England Biolabs) and purified by electrophoresis through 9% acrylamide-8 M urea and TBE (89 mM Tris, 89 mM borate, and 2 mM EDTA). The full-length template was electroeluted from the excized gel, precipitated, and resuspended in RNase-free Tris-EDTA buffer (10 mM Tris, and 1 mM EDTA, pH 7.0). The purified RNA was 5′ ^{32}P-labeled, electrophoresed on a sequencing gel, and autoradiographed to determine purity. The concentration of purified RNA was measured by UV spectrophotometrically at 260 nm, with the extinction coefficient 755 600 M^{-1} cm^{-1} (Dawson *et al.*, 1987), in the presence of 8 M urea.

The DNA primers listed in Table 1, which are complementary to the 3′ termini of the RNA 66-mer, were synthesized on an Oligo 1000 DNA synthesizer (Beckman). All DNA oligomers were purified by denaturing polyacrylamide gel electrophoresis (20% acrylamide, 8 M urea) and concentrations determined by UV absorbance at 260 nm. Before annealing, DNA primers were 5′ ^{32}P-labeled with T4 polynucleotide kinase (New England Biolabs) according to manufacturer's instructions. Unincorporated nucleotides were removed using a Biospin-30 column (Bio-Rad).

The duplex primer/templates of DNA/RNA were formed by annealing primers and templates at the molar ratio of 1.0:1.1. Prior to annealing, mixtures were denatured at 85 °C for 5 min, and then cooled slowly to room temperature in 2 h. To ensure that annealing had taken place, the duplex mixtures were analyzed by nondenaturing polyacrylamide gel electrophoresis (20%).

The DNA/DNA 25/45-mer duplex used in our work was adopted from Kati *et al.* (1992). It was purified and annealed according to their procedure.

Buffers. HIV-1 RT was preincubated with DNA/RNA substrates in buffer containing 50 mM Tris acetate (pH 7.5 at 37 °C), 100 mM potassium acetate, 0.1 mM EDTA. All reactions, except where indicated, were carried out in Mg^{2+} buffer containing 50 mM Tris acetate (pH 7.5 at 37 °C), 10 mM magnesium acetate, 100 mM potassium acetate, and 0.1 mM EDTA.

Rapid-Quench Experiments. Rapid-quench experiments were carried out in an apparatus designed by Johnson (1986) and built by KinTek Corporation (State College, PA). The apparatus contained a computer-controlled stepping motor and was modified for using small reaction volumes (15 μL). Typically, the experiments were carried out by loading the enzyme solution in one loop (15 μL) and the substrate solution in the second loop (15 μL) of tubing. The reactions were started by rapidly mixing the two solutions and quenched with 0.3 M EDTA (final concentration) after time intervals ranging from 3 ms to several minutes. Unless noted otherwise, all concentrations refer to concentrations during the reaction after mixing.

Pre-Steady State Kinetic Analysis for Incorporation of Next Correct Nucleotide to DNA/RNA Duplex at 37 °C. The pre-steady-state kinetic analysis was conducted under the conditions where the DNA concentration was in slight excess relative to the enzyme concentration. The reactions were carried out by mixing a solution containing the preincubated complex of 60 nM HIV-1 RT and 5′-labeled 200 nM DNA/RNA duplex with a solution of 10 mM Mg^{2+} and 100 μM dNTP. Polymerization was quenched with 0.3 M EDTA at time intervals ranging from 6 ms to 7 s. DNA products were quantitated by sequencing gel analysis. The product formation occurred in a fast phase followed by a slow phase. The data were fitted to a burst equation (see below).

Nitrocellulose-DEAE Membrane Double Filter Binding Assay at 23 °C. The procedures were adopted from Wong and Lohman (1994). Filter binding was carried out using a 96-well dot-blot apparatus, nitrocellulose, and DEAE membranes from Schleicher and Schuell. This assay is based on that the nitrocellulose membrane retains RT·DNA/RNA and the DEAE membrane traps all remaining DNA/RNA duplexes.

Wild-type RT (45 nM) was preincubated with increasing concentrations of DNA/RNA duplex in binding buffer (50 mM Tris acetate, 100 mM potassium acetate, 0.1 mM EDTA, pH 7.5 at 23 °C). Immediately prior to filtering each sample, the well was washed with 100 μL of binding buffer. With the vacuum applied, 25 μL of each sample was added to the well followed by 100 μL of buffer. This was repeated three times for each DNA/RNA duplex concentration. Following titration, substrate binding was quantitated using a Betascope 603 blot analyzer (Betagen, Waltham, MA).

Product Analysis. The products were analyzed by sequencing gel electrophoresis (10−20% acrylamide, 8 M urea, 1× TBE running buffer) and the products were quantitated using either a Betascope 603 blot analyzer (Betagen, Waltham, MA) or a 445 SI Phosphorimager (Molecular Dynamics, Sunnyvale, CA).

Data Analysis. Data were fitted by nonlinear regression using the KaleidaGraph program (Synergy Software, Reading, PA). Data from burst experiments were fitted to a burst equation: $[\text{product}] = AE_0[1 - \exp(-k_1t) + k_2t]$, where A represents the enzyme amplitude, E_0 the enzyme concentration measured spectrophotometrically, k_1 the observed burst rate, and k_2 the observed steady state rate. The biphasic kinetic data were fitted to a double exponential equation: $[\text{product}] = E_0A_1[1 - \exp(-k_1t)] + E_0A_2[1 - \exp(-k_2t)]$, where E_0 represents the total enzyme concentration measured spectrophotometrically, A_1 the fast-phase enzyme amplitude, k_1 the observed fast-phase rate, A_2 the slow-phase enzyme amplitude, and k_2 the observed slow-phase rate. The single-phase kinetic data were fitted to a single exponential equation: $[\text{product}] = E_0A[1 - \exp(-kt)]$, where E_0 represents the enzyme concentration measured spectrophotometrically, A the enzyme amplitude, and k the observed rate. Data from the active site titration and nitrocellulose-DEAE double filter binding assay were fitted to a quadratic equation: $[\text{E·DNA}] = 0.5(K_d + E_0 + D_0) - 0.5[(K_d + E_0 + D_0)^2 - 4E_0D_0]^{1/2}$, where K_d represents the equilibrium dissociation constant for DNA substrate, E_0 the active enzyme concentration, and D_0 the DNA concentration. The kinetic data for incorporation of three dATPs into duplex DNA/RNA 25/66-mer were modeled using the KINSIM kinetic simulation program provided by Carl Frieden and Bruce Barshop, Washington University, St. Louis, MO (Barshop *et al.*, 1983) as modified by Anderson *et al.* (1988) to accept *x-y* data pairs. Final fitting of the data was accomplished by nonlinear regression based upon kinetic simulation using a modification of the program FITSIM (Zimmerlie & Frieden, 1989).

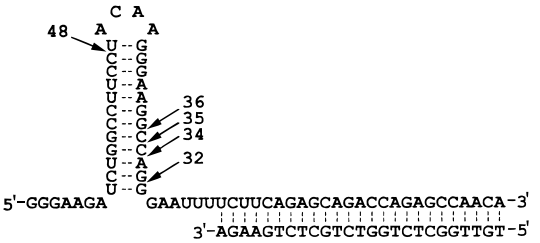

FIGURE 1: DNA/RNA 25/66-mer heteroduplex. The RT pause sites are numbered from the 3′ terminus of the 66-mer and are labeled by arrows.

RNA Folding. Computer program *Mfold* was used to locate secondary structures of HIV-1 genome and to calculate the thermodynamic parameters of optimal and suboptimal secondary structures. *Mfold* was based on the energy minimization method of Zuker (1989) and the energy values developed by Jaeger *et al.* (1989). *Mfold* is accessible on the internet at the uniform resource locator http://ibc.wustl.edu/∼zuker/.cgi.

RESULTS

Design of the Short RNA Template Containing a Stable Secondary Structure Derived from HIV-1 Genome. For our analysis of polymerase pausing, we searched for an appropriate RNA template that would form a stable secondary structure, without interior loops or bulges, and that was part of the HIV-1 RNA genome and less than 100 nucleotides in length. We used an RNA folding program *Mfold* to locate secondary structures of the entire HIV-1 RNA genome, and the most stable structure was selected (Figure 1). This hairpin structure is at least 4.6 kcal/mol more stable than the suboptimal structures, and its folding free energy is −20.3 kcal/mol at 37 °C as predicted by *Mfold*. It is stable because it has a GC-rich stem and a four nucleotide loop, which is the most stable loop size (Groebe & Uhlenbeck, 1988). We selected nucleotide 1636 of HIV-1 RNA genome as the first nucleotide on the 5′ terminus of the template (Ratner *et al.*, 1985); this resulted in an overhang of a few nucleotides that would stabilize the RNA hairpin structure and provide three rGs on the 5′ terminus that would increase transcriptional efficiency (Milligan & Uhlenbeck, 1989). Nucleotide 1701 was chosen as the 3′ terminus of the template so as to provide a sufficient length of RNA to form a DNA/RNA duplex with a 25 base DNA primer while leaving a six nucleotide gap between the 3′ terminus of the DNA primer and the stem of the hairpin structure (Figure 1). This 66 nucleotide template was synthesized by runoff transcription by T7 RNA polymerase, yielding more than 100 full-length RNA molecules per template molecule.

Processive Incorporation of Three dATPs at 37 °C. We analyzed the kinetics of three consecutive dATP incorporations from the 25 base primer in order to determine the kinetics of DNA synthesis while filling in the gap before the polymerase reached the base of the hairpin. The experiment was performed with 5′-labeled 25/66-mer (100 nM) in excess over enzyme (50 nM) under conditions where

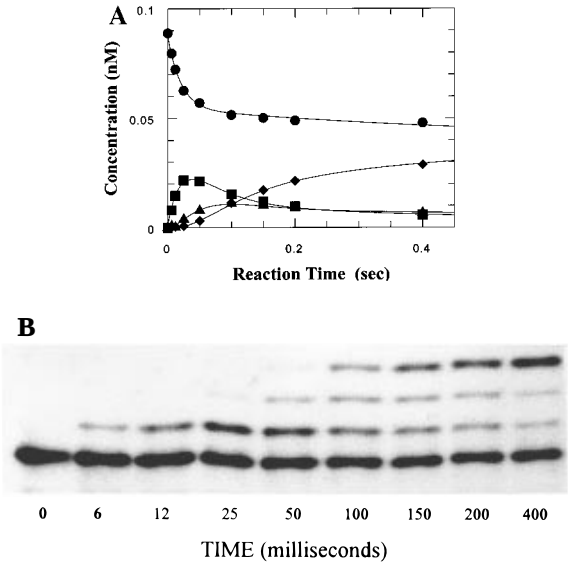

FIGURE 2: Kinetics of processive DNA synthesis. Three consecutive dATP incorporation reactions into 25/66-mer DNA/RNA were examined at 37 °C catalyzed by wild-type HIV-1 RT. A solution of RT (50 nM) was incubated with 5′ ^{32}P-labeled 25/66-mer (100 nM) and then reacted with dATP (100 μM) at 37 °C in buffer containing Mg^{2+} (10 mM) (final concentrations) for the indicated times. The reactions were quenched with 0.3 M EDTA and analyzed on a sequencing gel. Panel B shows the autoradiography of the products and substrate. The data indicate formation of the 26-mer (■), 27-mer (▲), 28-mer (◆) and depletion of the substrate 25-mer (●). The solid lines represent best fits obtained from computer simulation (KINSIM) using a mechanism consisting of three single nucleotide incorporations at rates of 46.1, 13.5, and 18.0 s^{-1}, respectively; and DNA/RNA dissociations at rates of 0.5, 3.3, 4.6, and 1.5 s^{-1}, respectively; and RT·DNA/RNA associations at rates of 38.6, 291.6, 143.8, and 72.0 μM^{-1} s^{-1}, respectively.

the measured kinetics of sequential elongation steps were due to a single enzyme binding event. The time courses for formation of elongated products and disappearance of substrate were fit using KINSIM to a mechanism consisting of three single nucleotide incorporation reactions, allowing dissociation of the enzyme from the DNA/RNA duplex before and after each step to account for the accumulation of intermediates. The simulated results shown in Figure 2 fit to consecutive rates of dATP incorporation of 46, 14, and 18 s^{-1} and average rate of DNA dissociation from the enzyme of 2.5 ± 1.5 s^{-1}. According to this fit, the average processivity of RT was calculated to be about 10. These results are similar to those obtained by analysis of five consecutive nucleotide incorporation reactions by Kati *et al.* (1992) using a DNA/DNA 25/45-mer substrate. This indicates that the effect of RNA secondary structure on DNA synthesis is not significant before RT reached the hairpin even though the final incorporation was only three nucleotides away from the base of the hairpin. The slower rate of incorporation observed for the second and third incorporation reaction (14 and 18.0 s^{-1}) may be a function of changes in DNA/RNA structure due to three consecutive A/U base pairs. However, these rates are within the normal range of variation in the rate of polymerization catalyzed by RT.

Kinetics of Polymerization at Pause and Nonpause Sites. When all four nucleotides are added to the reaction mixture, the polymerase proceeds through the hairpin to produce full-length 66-mer product, but the reaction is slow and several intermediates accumulate, identifying the pause sites summarized in Figure 1 (Suo & Johnson, 1997b). The accumulation of intermediates suggests that the kinetics of polymerization are significantly affected at particular locations while RT is reading through the template hairpin structure. To investigate the mechanistic basis for pausing, we performed pre-steady-state kinetic analysis of single nucleotide incorporation at each pause site and at several nonpause sites as described in Materials and Methods. Primers of different length were synthesized as shown in Table 1, annealed to the 66-mer RNA template, and used to examine the kinetics of single nucleotide incorporation. Accordingly, this series of template primer pairs allowed detailed analysis of the kinetics of polymerization at each pause site.

The time course of formation of products at each nonpause site shows a burst phase followed by a linear phase. The data were fitted to a burst equation. The primary data mirror that described previously (Kati *et al.*, 1992) and are not shown; the rates of polymerization obtained by fitting the data are summarized in Table 2. For example, the incorporation of dCTP as the next nucleotide using the 37/66-mer substrate occurred at a rate of 78 s^{-1} and with an enzyme amplitude of 64% in the burst phase and 0.04 s^{-1} in the linear phase. The fast burst phase of the reaction represents the rapid formation of product at the polymerase active site, while the linear phase is a function of the slow release of the product from the enzyme. This is typical of the reaction kinetics seen at nonpause sites.

In contrast, the time courses of product formation at pause sites exhibited low burst amplitudes (4−30%) and high rates of the slow phase (0.20−0.59 s^{-1}) as described below. According to the standard explanation of the burst kinetics,

Table 2: Kinetic Constants and Binding Affinity of Wild-Type HIV-1 RT

substrate	fast rate (s^{-1})	amplitude (%) (fast phase)	slow rate (s^{-1})	amplitude (%) (slow phase)	K_d (nM) (polymerase site)	K_d (nM) (overall)
20/66-mer	62 ± 4	62.9 ± 1.0			8.3 ± 0.6	15.4 ± 1.1
25/66-mer	46[a]				13[a]	27.5 ± 4.6
26/66-mer	14[a]				11[a]	
27/66-mer	18[a]				32[a]	
28/66-mer					21[a]	
32/66-mer	75 ± 13	15.1 ± 0.6	0.4 ± 0.2	10.9 ± 0.8	105 ± 12	31.5 ± 3.1
35/66-mer	54 ± 20	5.5 ± 0.5	0.17 ± 0.01	39.3 ± 0.6	171 ± 23	35.5 ± 5.6
36/66-mer	71 ± 19	10.0 ± 0.5	0.07 ± 0.01	24.9 ± 1.1	44.5 ± 3.0	38.4 ± 3.6
37/66-mer	78 ± 6	66.1 ± 2.0			4.0 ± 0.8	8.8 ± 1.0
47/66-mer	61 ± 8	24.9 ± 0.9	0.49 ± 0.09	22.3 ± 1.0	12.6 ± 1.5	19.4 ± 2.9
48/66-mer	76 ± 18	4.0 ± 0.2	0.09 ± 0.01	19.6 ± 0.6	290 ± 33	16.8 ± 3.5

[a] The data are obtained from Figure 2, and the K_d values were calculated using the dissociation rates divided by their corresponding association rates. The substrates corresponding to the strong pause sites are in bold-type.

the rate of the slow phase observed at the pause sites could be due to the faster dissociation of DNA products from the enzyme after the single nucleotide incorporation (Kati *et al.*, 1992). To test this postulate, we measured directly the rate of dissociation of the 48/66-mer from RT by the following method. A solution of 5′-labeled 48/66-mer (100 nM) was incubated with RT (75 nM) for 30 min to form the enzyme−48/66-mer complex. This solution was then mixed with unlabeled DNA/DNA 25/45-mer (5 μM) and incubated for periods of 8−65 s, such that the labeled 48/66-mer would dissociate from the enzyme and be replaced by the unlabeled 24/45-mer. At various times, a solution of 10 mM Mg^{2+} and 100 μM dCTP was added to initiate polymerization and then the reaction was stopped with 0.3 M EDTA after a constant interval of 10 s, sufficient to allow the conversion of any 48-mer to either a 49-mer or a 50-mer. The products were analyzed by sequencing gel electrophoresis. The time course of the total products followed a single exponential with a rate of 0.042 ± 0.008 s^{-1} (data not shown). This represents the rate of dissociation of the 48/66-mer from the polymerase active site. The time allowed for the polymerization reaction (10 s) is sufficiently short that the slower reactions do not contribute to the amount of products. The estimated rate of 0.04 s^{-1} for the dissociation of the 48/66-mer from the enzyme is much smaller than the rate of 0.59 s^{-1} measured from slow phase of the polymerization reaction; therefore, the slow phase must be due to some reaction other than dissociation of the DNA product from the enzyme. Indeed, the dissociation rates of all substrates (0.04 ± 0.01 s^{-1}) measured from our analysis of the RNase H activity described in the following paper in this issue (Suo & Johnson, 1997a) further support this conclusion.

An alternate pathway could account for the higher rates of the slow phase of polymerization observed at the pause sites. The low amplitude of the fast reaction phase and the observed rate of the slow phase could be a function of two modes of binding of the DNA/RNA substrates to the enzyme. According to this model, the small amplitude of the fast reaction is a function of a small fraction of the DNA/RNA bound productively to the enzyme at the polymerase site. The remainder of the DNA/RNA is then slowly converted to the productive mode without dissociation from the enzyme, allowing polymerization to occur. If this mechanism were correct, incorporation of the next nucleotide in a single enzyme binding event should follow biphasic kinetics at each pause site. To examine this pathway, we measured the kinetics of next nucleotide incorporation in a single turnover in the presence of an excess DNA trap to sequester free enzyme. A solution of 5′-labeled 36/66-mer was incubated with RT and then was mixed with a solution of Mg^{2+} and dCTP to initiate the polymerization reaction in the presence of a large molar excess of unlabeled DNA/DNA 25/45-mer. The unlabeled 25/45-mer served as a trap for free RT to prevent rebinding of the 36/66-mer. The polymerization reaction was quenched with 0.3 M EDTA at time intervals ranging from 6 ms to 60 s, and the reaction products were analyzed on a sequencing gel. The resulting time course of product formation follows biphasic kinetics (Figure 3). The data were fitted to a double exponential equation (see Materials and Methods). The fast phase occurred at a rate of 71 s^{-1} with a reaction amplitude of 10.0%, while the slow phase occurred at a rate of 0.07 s^{-1} with an amplitude of 24.9%, relative to the enzyme concentration. Similar experiments were performed at other pause sites to get the results summarized in Table 2. The observation that the incorporation of the next nucleotide at all pause sites followed biphasic kinetics in the presence of excess unlabeled DNA indicates that the DNA must bind to the enzyme in two modes, one reacting rapidly and another reacting slowly.

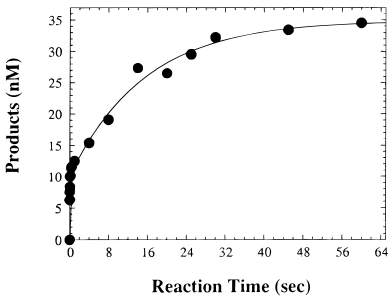

FIGURE 3: Biphasic polymerization kinetics at pause sites. The incorporation of dCTP into 36/66-mer DNA/RNA was examined at 37 °C. A solution of RT (100 nM) was incubated with 36/66-mer (100 nM) and then was mixed with dCTP (100 μM), unlabeled 25/45-mer (5 μM), and Mg^{2+} (10 mM). The reactions were quenched at the time intervals ranging from 6 ms to 60 s by the addition of 0.3 M EDTA. DNA products were quantitated by sequencing gel analysis. The data were fitted to a double exponential equation, which gave a fast rate of 71 s^{-1} with an amplitude of 10.0%, and a slow rate of 0.07 s^{-1} with an amplitude of 24.9%, relative to the enzyme concentration.

When a similar experiment was performed with primers at nonpause sites such as the 20 and 37-mer, we observed only the large amplitude fast phase of the polymerization reaction. The time courses of product formation were fitted to a single exponential equation, and the resulting kinetic data shown in Table 2 agree with those obtained previously. These results demonstrate that the mechanisms of nucleotide incorporation at pause and nonpause sites are different and, in particular, the kinetics of incorporation at pause sites are biphasic indicating two rates of polymerization. Moreover, since the fast and slow rates of polymerization were observed in the presence of added trap DNA, both reactions occur without dissociation of the DNA/RNA duplex from the enzyme.

Measurement of the Affinity of Substrates at the Polymerase Site of RT by Active Site Titration at 37 °C. As shown in Table 2, the enzyme amplitudes in the fast phase are very different at pause and nonpause sites. This demonstrates that the binding of DNA substrates at the polymerase site is affected by the template hairpin. To verify this conclusion, we measured the binding affinity of substrates at the polymerase site of RT. Because both the dissociation rate of the RT·DNA complex and the nucleotide incorporation rate in the slow phase are much smaller than the rate of polymerization in the fast phase, it is possible to estimate the affinity of substrates at the polymerase site of RT by examining the DNA concentration dependence of the amplitude of the fast phase. The amplitude of the fast phase corresponds to the percentage of RT which initially binds DNA substrates productively at the polymerase site in the solution allowing equilibration of RT + DNA with the RT·DNA complex. The active site titration was performed by incubating a fixed concentration of RT with increasing concentrations of 5′ ^{32}P-labeled DNA/RNA 36/66-mer at 37 °C. The amount of active RT·DNA complex present in solution was then measured by rapidly mixing it with a solution of dCTP and Mg^{2+} to allow a single turnover.

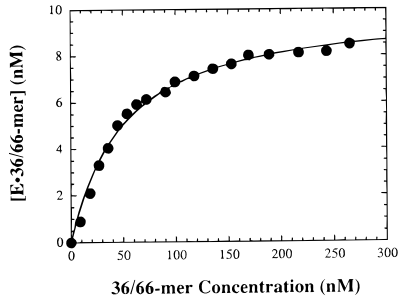

FIGURE 4: Active site titration of HIV-1 RT with 36/66-mer DNA/RNA duplex. RT (120 nM) was incubated with increasing concentrations of 5′ ^{32}P-labeled 36/66-mer and then mixed with a solution of dCTP (100 μM) and Mg^{2+} (10 mM) in a rapid quench apparatus. The reactions were quenched after 100 ms by 0.3 M EDTA. The data represent the burst amplitudes at the respective 36/66-mer concentrations (before mixing). The solid line is a fit of the data to the quadratic equation, which gave a K_d value for the RT•36/66-mer complex of 44.5 ± 3.0 nM, and an amplitude of 8.3 ± 0.2%.

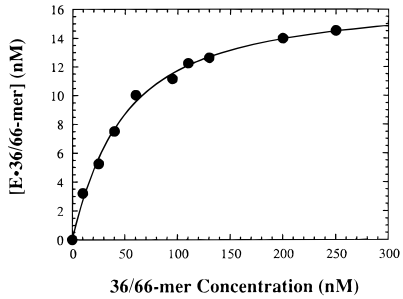

FIGURE 5: Total binding of the DNA/RNA 36/66-mer to HIV-1 RT. The K_d for formation of the RT•36/66-mer complex was measured using a nitrocellulose-DEAE membrane filter binding assay. RT (45 nM) was incubated with increasing concentrations of 5′ ^{32}P-labeled 36/66-mer and then applied to the wells of nitrocellulose and DEAE double-filter dot-blot apparatus. The solid line is a fit of the data to the quadratic equation, which gave a K_d value for the RT•36/66-mer complex of 38.4 ± 3.6 nM, and an amplitude of 39.3 ± 1.3%.

Reactions were quenched after 100 ms, which allowed adequate time to reach the maximum burst amplitude with negligible contribution of multiple turnovers or the slow reaction phase. The dependence of the enzyme amplitudes on the 36/66-mer concentration (before mixing) is shown in Figure 4. The solid line is a fit of the data to the quadratic equation, which gives a K_d for the RT•36/66-mer complex of 45 ± 3 nM.

The similar active site titration was conducted with primers of 20, 32, 35, 37, 47 and 48 nucleotides in length and the results are summarized in Table 2. These results clearly show that DNA substrates are bound tightly to the polymerase site of RT at nonpause sites and somewhat more weakly at pause sites.

Measurement of Overall Affinity of DNA by Nitrocellulose-DEAE Double Filter Binding Assay at 23 °C. The kinetic evidence presented above indicates that DNA binds to RT in both a productive and nonproductive mode at the pause sites. Since the active site titration described above (Figure 4) measured only DNA binding in the productive mode, it was necessary to use a method that measured total DNA binding to the enzyme. At the pause sites, DNA remains bound to RT during the slow phase of the reaction and dissociates slowly from RT and therefore, a method that measured total DNA binding should provide a sum of the two binding modes, but with the same observed affinity (see Appendix). To test this hypothesis, we measured the overall binding affinity of DNA to RT using nitrocellulose-DEAE double filter binding assay (see Materials and Methods). After allowing equilibration of 45 nM RT with increasing concentrations of 5′-labeled 36/66-mer, the samples were applied to the double filters. After washing with buffer three times, the nitrocellulose membrane retains RT•36/66-mer and the DEAE membrane traps all remaining 36/66-mer duplexes. Figure 5 shows the average concentrations of RT•36/66-mer retained by the nitrocellulose after correction for nonspecific retention of free DNA against the total concentrations of 36/66-mer. The data were fitted to a quadratic equation, which gave a K_d for RT•36/66-mer complex of 38 ± 4 nM. Thus, both methods of measuring binding affinity provided the same value. DNA/RNA duplexes consisting of the 20/66-mer, 25/66-mer, 35/66-mer, 47/66-mer, and 48/66-mer were examined using the filter binding assay and data are summarized in Table 2. In three cases (the 32-mer, 35-mer, and 48-mer), the K_d for binding to the polymerase site measured by the active site titration was larger than the K_d for total DNA binding measured by the nitrocellulose assay. The significance of this difference is not clear. In the case of the 35/66-mer and the 48/66-mer, this discrepancy could be due to the inaccuracies in measuring such small burst amplitudes (4−5%).

The similar overall binding affinity of substrates suggests that the RNA secondary structure does not significantly alter the binding of DNA/RNA duplexes to the binding cleft of RT, though it does affect binding at the polymerase active site. This conclusion is supported by our RNase H activity studies (see Suo & Johnson, 1997a).

DISCUSSION

Kinetics of DNA Synthesis Close to the Secondary Structure. The rate-limiting step for each nucleotide incorporation with linear DNA and RNA templates is the enzyme conformational change prior to the chemistry step, and following the chemical reaction, the translocation step is fast (Kati *et al.*, 1992). The data defining three consecutive dATP incorporation reactions shown in Figure 2 were fit by nonlinear regression to the same mechanism as in Figure 6 of Kati *et al.* (1992). The average processivity of three dATP incorporations, calculated to be 10, was similar to the value of 10−20 observed by Kati *et al.* (1992) using linear DNA and RNA templates. Thus, the kinetics of processive polymerization is not affected significantly even though the RNA secondary structure is very close to the 3′ terminus of the primer. This result indicates that the melting of the RNA hairpin structure probably has not yet begun since RT did not pause during the consecutive incorporation of three dATPs. Interestingly, the polymerase did not pause until it reached the stable base pairs in the stem of the hairpin, suggesting that the polymerase active site is able to accommodate the hairpin adjacent to the site of nucleotide incorporation.

Kinetics at Pause and Nonpause Sites. While RT is reading through the template secondary structure, one base pair of secondary structure has to be melted each time RT translocates to the next position. Because each melting step costs energy, several pause sites in the stem of the hairpin were identified and the location of the pause sites is directly correlated with the energy barrier for melting at each position

(Suo & Johnson, 1997b). A pause site (48/66-mer) appearing in the loop of the hairpin was also identified, and it is due to the rapid formation of a new hairpin structure occurring during the progress of DNA polymerization through the hairpin. This new hairpin has a seven nucleotide loop and a seven base pair stem. The pause site is relocated to the beginning of the hairpin stem (Suo & Johnson, 1997b). In this report, we have defined the changes in the kinetics of polymerization that are affected significantly by the template secondary structure at each site.

At the nonpause sites, the kinetics of next nucleotide incorporation occurred by a single exponential, followed by a slow linear phase which is a function of steady state turnover, limited by the release of the DNA from the enzyme. The high reaction amplitude (66%), the small dissociation rate (0.04 s^{-1}), and the high binding affinity at the polymerase site (4 nM) of duplex 37/66-mer (Table 2) were similar to that observed using a linear RNA template by Kati *et al.* (1992). These data are also similar to the data obtained using duplex 20/66-mer with the secondary structure far away from the 3′ terminus of primer (Table 2). These data indicate that most of enzyme molecules are active and that the duplex 37/66-mer is bound productively at the polymerase site. Therefore, the 37 nucleotide primer was quickly elongated to 38-mer and if all four nucleotides were added to the solution, the 37-mer would not accumulate. This is consistent with accumulation pattern shown in Figure 2 of Suo and Johnson (1997b). The somewhat higher reaction amplitudes observed with 20/66-mer and 37/66-mer than that obtained by Kati *et al.* (1992) may be a result of improved RT purification employed here.

In contrast to the results seen at the nonpause sites, the incorporation of the next nucleotide at each of the pause sites (32/66-mer, 35/66-mer, 36/66-mer, 47/66-mer, and 48/66-mer) exhibited biphasic kinetics that were a function of two modes of binding the DNA/RNA duplexes to RT. The data summarized in Table 2 indicate that the fast incorporation rates of substrates with primers 32, 35, 36, and 48 nucleotides in length are similar to those of 20/66-mer and 37/66-mer. This suggests that the rate-limiting step in the fast phase is similar to that described previously (Kati *et al.*, 1992). However, the reaction amplitudes of the fast phase (4.0−15%) are significantly smaller than those observed with the 37/66-mer and 20/66-mer. This indicates that only a small fraction of the enzyme−DNA complex was able to rapidly catalyze the DNA synthesis. In contrast, the slow phase of the reaction revealed that a larger portion of enzyme molecules (10−40%) were involved in the slow catalysis at the rates of 0.07−0.40 s^{-1}. The total reaction amplitude summing the fast and slow phases is still smaller than that observed of 20/66-mer or 37/66-mer, suggesting that some of the nonproductively bound substrates may be released from the enzyme prior to participating in the polymerization reaction.

Each of the observed differences in polymerization kinetics contributes to the strong accumulation of intermediate products (32, 35, 36, and 48-mer) shown in Figure 1 (Suo & Johnson 1997b). The 48/66-mer exhibited the smallest reaction amplitude (4%) in the fast phase of all primer/template substrates examined. This analysis provides an explanation for the strong pausing of RT after synthesis of the 48-mer, especially at 8 °C (Suo & Johnson, 1997b). Although incorporation of dATP to extend the 47-mer to a 48-mer exhibits biphasic kinetics, the larger reaction amplitude (25%) of the fast phase and the larger rate of the slow phase (0.5 s^{-1}) account for the minor accumulation of product 47-mer (Suo & Johnson, 1997b) as compared to the same parameters measured at the strong pause sites.

Scheme 1

$$\begin{array}{ccc} E + D_n & \overset{K_1}{\rightleftharpoons} & E{\cdot}D_n^N \\ \uparrow\downarrow & & \uparrow\downarrow K_2 \\ E + D_n^P & \rightleftharpoons & E{\cdot}D_n^P \xrightarrow[dNTP]{fast} E{\cdot}D_{n+1}{\cdot}PP_i \end{array}$$

During processive synthesis in the presence of all four nucleotides, there was a strong accumulation of products 35 and 36 nucleotides in length indicative of pausing at these sites, but there was no accumulation of the 37-mer. The kinetic data obtained by analysis of single nucleotide incorporation and summarized in Table 2 provide a quantitative explanation of these observations. Each of the 35/66 and 36/66 nucleotide substrates bind weakly to the polymerase site and show biphasic polymerization kinetics, with a large, slow reaction phase, accounting for the accumulation of 35-mer and the 36-mer. In contrast, very different results were obtained with duplex 37/66-mer, which does not accumulate. When the 37/66-mer was used as a substrate, the rate of single nucleotide incorporation was fast, corresponding to that which is seen with linear RNA templates. Accordingly, these data explain the absence of the accumulation of the 37-mer and provide additional evidence for the change in RNA secondary structure to form the smaller, downstream hairpin (Suo & Johnson, 1997b).

Tight Binding of All Substrates at the Binding Cleft of HIV-1 RT. It was quite surprising that all substrates bound to RT with a relatively high affinity. The crystal structure data (Kohlstaedt *et al.*, 1992; Jacobo-Molina *et al.*, 1993), the chemical footprinting data (Metzger *et al.*, 1993), and DNase I footprinting data (Wöhrl *et al.*, 1995) have revealed that HIV-1 RT has a larger than 19 base pair binding cleft that includes the polymerase and RNase H active sites. We speculate that this binding cleft is large enough to bind DNA tightly even in the presence of template secondary structure. This is confirmed by the high overall binding affinity of all tested substrates (8.8−38.4 nM) measured by the nitrocellulose-DEAE double filter binding assay (Table 2). Therefore, the template secondary structure does not significantly affect overall tight binding of DNA to RT although it dramatically alters the binding at the polymerase site of RT. The biphasic incorporation of next nucleotide at pause sites in a single turnover and the slow dissociation of all DNA substrates from the RT binding cleft described in the following paper in this issue (Suo & Johnson, 1997a) further support this conclusion.

The Mechanism of Pausing Due to Template Secondary Structure. The polymerization at pause sites can be described by the mechanism shown in Scheme 1. Initially, some DNA substrate molecules are bound productively at the polymerase site of RT ($E{\cdot}D_n^P$) with the next stem base pair melted and ready to rapidly accept the next nucleotide to form the elongated product. This reaction occurs at a rate of 50−80 s^{-1}. Other substrate molecules are bound nonproductively ($E{\cdot}D_n^N$) and are slowly converted to the productively bound state and are then turned over to products. This slow conversion of the DNA from the nonproductive to the productive state, without dissociation of the DNA from the

enzyme, accounts for the slow reaction phase. The structure of the enzyme−DNA complex in the nonproductive state cannot be ascertained from these kinetic studies, and the shift to the productive state could involve changes in structure of the enzyme, the DNA, or both. However, it is reasonable to suppose that the nonproductively bound substrate could have an intact next stem basepair which blocks the incorporation of next nucleotide. Thus, at pause sites, HIV-1 RT remains bound to DNA substrates waiting for the next stem base pair of template secondary structure to be melted and the conversion of the nonproductive to the productive state involves the melting out of the next stem base pair. In addition, when the 36/66-mer was used as a substrate, the conversion of nonproductive to productive state could result from the RNA secondary structure change (Suo & Johnson, 1997b).

Klarmann *et al.* (1993) have proposed two mechanisms to account for pausing. First, they propose that DNA dissociates from RT at the pause sites. Alternatively, they suggest that RT remains bound to the DNA substrates and that DNA polymerization occurs at a greatly reduced rate at pause sites. Our data show that all substrates have similar small dissociation rates as described in our following paper in this issue (Suo & Johnson, 1997a); therefore, release of the DNA from the polymerase site cannot account for the strong pause sites. However, dissociation of the DNA may account for pausing in most runs ($\geq$4 bases) of template deoxythymidines and deoxyadenosines during plus-strand synthesis on the DNA template (Klarmann *et al.*, 1993). This requires further investigation. Our results show that pausing is largely a function of the slower reaction occurring at the polymerase site. However, this is only part of the story in that our observation of biphasic polymerization kinetics at the pause sites implies two modes of DNA binding which are slowly interconverted.

Another feature of the unwinding process that we have described is the change in RNA secondary structure that occurs after the hairpin has been read through only halfway (Suo and Johnson, 1997b). This change in structure leads to the formation of a new hairpin downstream of the first, effectively destabilizing the major hairpin and thereby facilitating the unwinding and allowing the polymerase to efficiently read through the long 12 base pair stem.

The pattern of the predicted energy barriers of unwinding as a function of position through the hairpin correlates well with the product accumulation pattern in that the pause sites occur at positions with predicted high energy barriers for unwinding (Suo & Johnson, 1997b). This indicates that HIV-1 RT requires energy to traverse RNA secondary structure. The overall free energy change for single nucleotide incorporation catalyzed by T7 DNA polymerase at 20 °C was estimated to be −4 kcal/mol (Patel *et al.*, 1991), and a similar overall free energy change for single nucleotide incorporation catalyzed by HIV-1 RT is expected. This energy may be available as the driving force to unwind the next stem base pair. However, the most plausible stepwise base pair melting mechanism is the thermal breathing of individual stem base pairs followed by the rapid incorporation of the next nucleotide.

In conclusion, we have determined the kinetic basis for pausing during DNA synthesis through an RNA template containing a stable hairpin structure. Before reaching the template hairpin structure, the kinetics of processive polymerization is unaffected by the secondary structure and is similar to that using a linear DNA and RNA template without secondary structures. However, the kinetics of next nucleotide incorporation at the pause sites is very different. A small fraction of the DNA/RNA duplex is bound productively at the polymerase site and undergoes rapid extension upon the addition of the next correct base. A larger fraction of the DNA/RNA duplex is bound in a mode that can only be described as nonproductive and the slow conversion to a productive state limits the rate of polymerization. Thus, it appears that RT reads through RNA secondary structure by holding on to the template and waiting for the next base pair to unwind. It then catalyzes the extension of the DNA primer by rapid incorporation of the next base. Because RT has no proofreading activity, each step forward is largely irreversible, and the enzyme slowly progresses through the secondary structure, one step at a time. This process works because the polymerase active site is able to accommodate the hairpin adjacent to the site of polymerization. It will be important to examine the structural details of the active site of RT that allow the binding of the hairpin so close to the site of polymerization. If there are specialized structures of the protein responsible for binding the hairpin, they may be conserved providing an additional target for rational drug design.

ACKNOWLEDGMENT

The authors sincerely thank Dr. Roger Goody (Max-Planck Institute, Heidelberg) for providing the clone of wild-type HIV-1 RT (p66/p51).

APPENDIX

Derivation of Observed Equilibrium Dissociation Constants (K_d) of DNA Substrates Measured by the Active Site Titration and Nitrocellulose-DEAE Double Filter Binding Assay. In Scheme 1, the equilibrium constants K_1 and K_2 are $K_1 = [E{\cdot}D_n^N]/\{[E][D_n]\}$ and $K_2 = [E{\cdot}D_n^P]/[E{\cdot}D_n^N]$. Therefore, $[E{\cdot}D_n^N] = K_1[E][D_n]$, and $[E{\cdot}D_n^P] = K_1K_2[E][D_n]$. The total enzyme concentration in the preincubated solution of enzyme and DNA is $[E_0] = [E] + [E{\cdot}D_n^N] + [E{\cdot}D_n^P] = [E] + K_1[E][D_n] + K_1K_2[E][D_n]$. The active site titration measures the concentration of productively bound DNA ($E{\cdot}D_n^P$) but the double filter binding assay determines the concentration of both productively and nonproductively bound DNA ($E{\cdot}D_n^P$ and $E{\cdot}D_n^N$). For the active site titration, $[E{\cdot}D_n^P]/[E_0] = K_1K_2[E][D_n]/\{[E] + K_1[E][D_n] + K_1K_2[E][D_n]\} = K_1K_2[D_n]/\{1 + K_1(1 + K_2)[D_n]\} = A_1[D_n]/\{K_d + [D_n]\}$, where $A_1 = K_2/(1 + K_2)$, and $K_d = [K_1(1 + K_2)]^{-1}$. For the double filter binding assay, $\{[E{\cdot}D_n^N] + [E{\cdot}D_n^P]\}/[E_0] = \{K_1[E][D_n] + K_1K_2[E][D_n]\}/\{1 + K_1(1 + K_2)[D_n]\} = K_1(1 + K_2)[D_n]/\{1 + K_1(1 + K_2)[D_n]\} = [D_n]/\{K_d + [D_n]\}$, where $K_d = [K_1(1 + K_2)]^{-1}$. Therefore, the observed equilibrium dissociation constants of DNA substrates (K_d) measured by the two methods should be the same. The only difference resulting from the two different methods is the constant A_1, which is less than 1. This means the enzyme amplitude from the active site titration should be smaller than that measured by the double filter binding assay. The smaller the K_2, the smaller the value of A_1, and the smaller the amplitude obtained by the active site titration.

REFERENCES

Anderson, K. S., Sikorski, J. A., & Johnson, K. A. (1988) *Biochemistry 27*, 7395−7406.

Barshop, B. A., Wrenn, R. F., & Frieden, C. (1983) *Anal. Biochem. 130*, 134−145.

Dawson, R. M. C., Elliott, D. C., Elliott, W. H., & Jones, K. M. (1987) *Data for Biochemical Research*, Oxford University Press, NY.

Dudding, L. R., Nkabinde, N. C., & Mizrahi, V. (1991) *Biochemistry 30*, 10498−10506.

Groebe, D. R., & Uhlenbeck, O. C. (1988) *Nucleic Acids Res. 16*, 11725−11735.

Hansen, J., Schulze, T., Mellert, W., & Moelling, K. (1980) *EMBO J. 7*, 239−243.

Hoffman, A. D., Banapour, B., & Levy, J. A. (1985) *Virology 147*, 326−335.

Huber, H. E., Macoy, J. M., Seehra, J. S., & Richardson, C. C. (1989) *J. Biol. Chem. 264*, 4669−4678.

Jacobo-Molina, A., Ding, J., Nanni, R. G., Clark, A. D., Jr., Lu, X., Tantillo, C., Williams, R. L., Kamer, G., Ferris, A. L., Clark, P., Hizi, A., Hughes, S. H., & Arnold, E. (1993) *Proc. Natl. Acad. Sci. U.S.A. 90*, 6320−6324.

Jaeger, J. A., Turner, D. H., & Zuker, M. (1989) *Proc. Natl. Acad. Sci. U.S.A. 86*, 7706−7710.

Johnson, K. A. (1986) *Methods Enzymol. 134*, 677−705.

Kati, W. M., Johnson, K. A., Jerva, L. F., & Anderson, K. S. (1992) *J. Biol. Chem. 267*, 25988−25997.

Klarmann, G., Schauber, C. A., & Preston, B. D., (1993) *J. Biol. Chem. 268*, 9733−9802.

Kohlstaedt, L. A., Wang, J., Friedman, J., Rice, P. A., & Steitz, T. A. (1992) *Science 256*, 1783−1790.

Le Grice, S. F. J. (1993) in *Reverse Transcriptase* (Skalka, A. M., & Goff, S. P., Ed.) pp 163−192, Cold Spring Harbor Laboratory Press, Plainview, NY.

Milligan J. F., & Uhlenbeck, O. C. (1989) *Methods Enzymol. 180*, 51−62.

Muller, B., Restle, T., Weiss, S., Gautel, M., Sczakiel, G., & Goody, R. S. (1989) *J. Biol. Chem. 264*, 13975−13978.

Olsen, D. B., Carroll, S. S., Culberson, J. C., Shafer, J. A., & Kuo, L. C. (1994) *Nucleic Acids Research 22*, 1437−1443.

Patel, S. S., Wong, I., & Johnson, K. A. (1991) *Biochemistry 30*, 511−525.

Pop, M. P., & Biebricher, C. K. (1996) *Biochemistry 35*, 5054−5062.

Ratner, L., Haseltine W., Patarca, R., Livak, K. J., Starcich, B., Josephs, S. F., Doran, E. R., Rafalski, J. A., Whitehorn, E. A., Baumeister, K., Ivanoff, L., Petteway, S. R., Jr., Pearson, M. L., Lautenberger, J. A., Papas, T. S., Ghrayeb, J., Chang, N. T., Gallo, R. C., & Wong-Staal, F. (1985) *Nature 313*, 277−284.

Reardon, J. E. (1992) *Biochemistry 31*, 4473−4479.

Rey, M. A., Spire, B., Dormont, D., Barre-Sinoussi, & Chermann, J. C. (1984) *Biochem. Biophys. Res. Commun. 121*, 126−133.

Stahlhut, M., Li, Y., Condra, J. H., Fu, J. Gotlib, L., Graham, D. J., & Olsen, D. B. (1994) *Protein Expression Purif. 5*, 614−621.

Suo, Z., & Johnson, K. A. (1997a) *Biochemistry 36*, 12468−12476.

Suo, Z., & Johnson, K. A. (1997b) *Biochemistry* (manuscript submitted for publication).

Wöhrl, B. M., Tantillo, C., Arnold, E., & Le Grice, S. F. J. (1995) *Biochemistry 34*, 5343−5350.

Wong, I., & Lohman, T. M. (1993) *Proc. Natl. Acad. Sci. U.S.A. 90*, 5428−5432.

Zimmerlie, C. T., & Frieden, C. (1989) *Biochem. J.* 258, 381−387.

Zuker, M. (1989) *Science 244*, 48−52.

BI971217H